An Optimal Control Model for Analyzing Human Postural Balance

Arthur D. Kuo, *Member, IEEE*

Abstract—**The question posed in this study is whether optimal control and state estimation can explain selection of control strategies used by humans, in response to small perturbations to stable upright balance. To answer this question, a human sensorimotor control model, compatible with previous work by others, was assembled. This model incorporates linearized equations and full-state feedback with provision for state estimation. A form of gain-scheduling is employed to account for nonlinearities caused by control and biomechanical constraints. By decoupling the mechanics and transforming the controls into the space of experimentally observed strategies, the model is made amenable to the study of a number of possible control objectives. The objectives studied include cost functions on the state deviations, so as to control the center of mass, provide a stable platform for the head, or maintain upright stance, along with a cost function on control effort. Also studied was the effect of time delay on the stability of controls produced using various control strategies. An objective function weighting excursion of the center of mass and deviations from the upright stable position, while taking advantage of fast modes of the system, as dictated by inertial parameters and musculoskeletal geometry, produces a control that reasonably matches experimental data. Given estimates of sensor performance, the model is also suited for prediction of uncertainty in the response.**

I. Introduction

BIOMECHANICAL models of varying complexity have been used extensively in the study of mammalian coordination of movement, e.g., [9], [28], [4]. However, much of the current work in modeling has limited applicability to issues studied by motor control scientists. It is hoped that these models can be adapted and used to address specific issues in systems neurophysiology. Control of balance in human upright standing is particularly well-suited for modeling, and is also a popular experimental paradigm [26]. Human posture therefore serves as an ideal starting point for applying modeling to specific problems in motor control.

Investigators have reported that standing human subjects, when perturbed by backwards translation of a moving support surface and instructed not to move their feet, typically respond by moving in the sagittal plane, using one or a combination of two strategies [26]. For small disturbances [14], they tend to keep the knees, hips, and neck fairly straight, moving predominantly about the ankles (the "ankle strategy"). For disturbances that place their center of mass near the perimeter of foot support, they tend to use a motion coordinating flexion or extension of the hips with smaller concurrent extension or flexion of the ankles (the "hip strategy"), keeping the other joints fairly straight. These strategies have also been reported using ground reaction forces and electromyograms, but with some ambiguity of definition [1], [14], [26]. In this paper, analysis of these strategies is explicitly restricted to the kinematic definitions above.

Modeling of this experimental paradigm (disturbances to posture in the sagittal plane) is particularly convenient, as the dynamics can be linearized without significant impact on simulation accuracy, the motion is 2-D, and the response incorporates the three main components of sensorimotor control: detection, control, and actuation. For example, Hemami and colleagues [13], [11], [7] developed one- and two-link inverted pendulum models to study the use of constant state feedback gains to stabilize posture. They found that reasonable predictions of behavior can be made using linearized dynamics. They also computed minimal sets of stable feedback gains and performed system identification to find those gains.

Barin [3] used multiple regression to compute state feedback gains from experimentally derived kinematics, and found that a two-segment model, used with the computed feedback controls, is sufficient to accurately model and predict center-of-pressure excursion.

He *et al.* [10] developed a complex model of the cat neuro-musculo-skeletal system based on optimal (linear quadratic regulator) control. They used this model to analyze various control schemes, including joint position servo, muscle length servo, muscle stiffness, and full-state (mechanical states augmented with sensor and muscle states) feedback control.

There remains a gap, however, between these models and their application to issues in neural control of movement. For example, these models neither explain nor predict the selection of ankle and hip control strategies described in [26]. Linear models predict only scaled responses that vary with perturbation size; but human responses to large perturbations are not merely amplified responses to small perturbations [14]. Using "feasible acceleration sets," a method for characterizing the entire set of angular accelerations achievable about the joints, Kuo and Zajac [19], [20] found indications that biomechanical and control constraints play a role in forcing selection of strategies. As perturbations increase in size, subjects place greater reliance on the hip strategy, which also appears to be more effective in stabilizing the center of mass than the ankle strategy, even when constraints are inactive. Control models should therefore account for such constraints.

Manuscript received November 20, 1992; revised September 27, 1994. This work was supported in part by NIH grant NS178662, an NSF Predoctoral Fellowship, and the Rehabilitation Research and Development Service, Department of Veterans Affairs.

The author is with the Department of Mechanical Engineering and Applied Mechanics, University of Michigan, Ann Arbor, MI 48109-2125 USA.

IEEE Log Number 9406718.

Models (to date) also require complete state observability or measurability. For example, Hemami *et al.* [13], using simplified models, assumed that vestibular organs provide information concerning trunk angle, and joint proprioceptors information on lower body angles. He *et al.* [10] presumed the majority of states to be directly measurable by sensors. Joint angle information, by virtue of being observable, was presumed to be estimated by the CNS from muscle receptors. While the high redundancy of physiological sensors would strongly suggest full observability, it remains open to question whether the CNS actually performs the necessary calculations to provide full state information.

The question addressed here, then, is whether the modeling and control systems analysis techniques described above can be adapted to account for constraints. If so, will these new models provide an explanation for the selection of ankle and hip strategies? In addition, is there evidence in support of state estimation in the CNS, thereby justifying state feedback models?

Such explanation is naturally dependent on hypotheses concerning the objectives of the CNS. In experiments studying movement of the head, Allum *et al.* [2] have postulated that the selection of strategies may be driven partially by the desire to stabilize the head, where visual, and perhaps more importantly, vestibular sensors are located. McCollum and Leen [24] showed that stiffening the body so that it acts as a one-segment inverted pendulum (as in the ankle strategy) provides a longer time constant than if the body is stiffened as a two-segment inverted pendulum (as in the hip strategy). They concluded that the ankle strategy thereby provides greater chance of stability given transmission delays in the CNS controller. These delays may greatly affect children learning to stand, for whom mechanical time constants are smaller than, while transmission delays are similar to, those of adults. However, a controller has considerable flexibility in altering a system's eigenvalues (and hence, its time constants). Thus, the time constants of an uncontrolled pendulum may have little relation to those of the controlled system. The stability of the control (whether or not it is duplicating the behavior of a one- or two-segment inverted pendulum) is therefore not necessarily related to the time constants of inverted pendula.

The challenge, then, is to develop a model that is compatible with and builds upon the modeling work of others, and that can account for the constraints described in [19], [20], all within the framework of a control systems analysis. In this paper, a constraint-based state-feedback model is presented, in which control strategies can be incorporated in the objective equation. The relative efficacy of the ankle and hip strategies can thus be tested in relation to their ability to satisfy various objectives. The objectives tested include minimization of "neural effort," along with stabilization of the center of mass [20], and the head [2]. The resulting controllers are tested for satisfaction of constraints, settling time, and tolerance to transmission delays [24]. Moreover, arguments for the incorporation of state estimators in the optimal control model are presented, based on similar research on vestibular function in movement perception [27]. This model is substantially compatible with and integrates the work of others, and is ideally suited to examining issues raised in the experimental study of posture.

This paper is presented in five sections. In Section II, the requirements of the model and the foundation for its development are laid out. The mathematical formulation of the model is given in Section III. An objective function for simulating human responses is determined and tested in Section IV. The results are discussed and future work outlined in Section V.

II. Model Specifications and Rationale

Development of a model that can be applied directly to experimental paradigms requires that both model and experiment share certain features. These features, as outlined below, serve both as assumptions about the experimental conditions and as specifications the model must meet.

A. Input-Output Behavior

The motor control system is presumed to receive a desired state vector, x_d, from higher levels of the CNS, compare it with the measured state, and generate the motor command u, as shown in Fig. 1(a). Joint torques produced by the muscles and external forces produced by disturbances, lumped together in the vector T, act upon the body, resulting in movement described by joint angles, velocities, and accelerations (vectors θ, $\dot{\theta}$, and $\ddot{\theta}$, respectively). Because these (kinematics θ, $\dot{\theta}$, $\ddot{\theta}$, and the torques/forces T) are the only variables which can be reliably measured (or estimated) for comparison to a model, they will serve as the ideal inputs and outputs for a CNS controller model. The first requirement for the model is that it adequately represents the *input-output behavior* of the human system comprised of sensors, controller, and actuators. We will not concern ourselves with the actual information internal to that system (such as the internal coding of the state or motor commands), because those instruments that provide such information generally provide indirect or ambiguous data. For example, electromyograms provide indicators of the motor commands or muscle forces, but are affected by muscle shortening velocities, cross-talk, and various nonlinearities [34]. Electrodes in various locations can provide indicators of cortical, sensory, and other functions, but the sheer quantity of information makes it difficult to ascertain the meaning of the data, much less the actual "state representation."

B. Linearity

Because the body dynamics have been demonstrated to be fairly linear in this region [13], and (for a given perturbation) the closed-loop system comprised of both the controller and the body dynamics appears to be linear [3], the controller can be expected to behave linearly as well. Using multi-input multi-output transfer-function matrix, the model can therefore be analyzed using the rich set of tools from linear system theory. It is assumed that the CNS, though comprised of many nonlinear neural elements, will behave linearly about the operating point corresponding to upright static standing. Nonlinearities seen over a range of perturbation magnitudes are modeled using constraints [20], and are addressed through

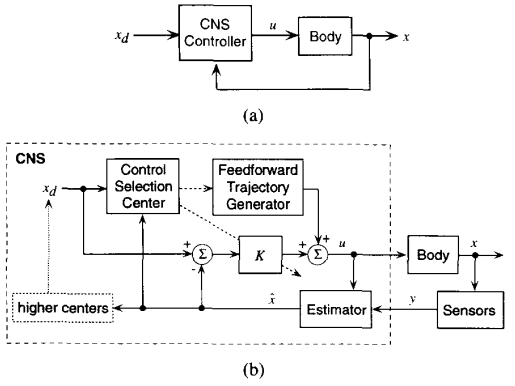

Fig. 1. (a) Diagram of feedback system. Central nervous system (CNS) produces control signals acting on the body. Resulting motion is fed back to controller. (b) Gain-selecting model accepts desired state x_d from higher centers, control selection center triggers a feedforward trajectory or set of feedback gains (or both). Body performs according to command signals, and motion is detected by sensors. State estimator uses efference copy u and sensory information y to form the state estimate $\hat{x}$ used by the lower level regulator or higher centers.

selection of specific linear controllers for each perturbation (see Section II-E).

C. Full-State Feedback

Studies of minimal sets of state feedback have shown that a controller requires less than a full set of mechanical states to stabilize the body [9], [7]. However, full-state feedback appears to provide the best match to experimental results [3]. He *et al.* [10] demonstrated observability of the states and found that full-state feedback used in the objective function produced the best stabilizing control of cat posture.

Experimental evidence also suggests that full-state information is available and is used in selection of control strategy. In order to discriminate between disturbances small enough to be countered by the ankle strategy, and those large enough to require the hip strategy, the CNS must have information from both lower and upper body sensors to estimate the motion of the center of mass [23]. However, stabilization is possible given only a subset of complete sensory information. For example, experiments have been performed in which the support surface is either rotated or translated backwards so as to produce similar ankle disturbances, hence rendering somatosensory information from the ankles and feet unreliable [1]. Proper stabilization by subjects demonstrates that upper-body sensors are sufficient to differentiate the two types of disturbance, that ankle joint information is not used exclusively in determining the response, and that there exists a feedback path from upper-body sensors to the leg muscles. Patients with vestibular deficits, on the other hand, are also able to withstand disturbances, indicating that utilization of ankle or foot somatosensors alone is sufficient for stability [15].

It is therefore assumed that all of the rigid body mechanical states, in an arbitrary realization, are available to or estimated by the CNS for use in forming a control response. The actual state realization used by the CNS is unimportant in this paper; of more importance is the input-output transfer-function matrix behavior, which is independent of realization [17]. The issue of how the state information is acquired is addressed in Section II.

D. Feedforward and/or Feedback

Some researchers have suggested that response to a disturbance is in the form of a feedforward trajectory, i.e., a motor tape that is played based on the sensory input, e.g., [25]. Others have proposed that the response is in the form of direct state feedback [3]. The proposed model maintains compatibility with both schemes in any combination (see Fig. 1(b)). In order to choose the correct response, a *control selection center* uses the mechanical state to select the type and amount of response necessary to counter the disturbance. This center evaluates the difference between an estimated state and the desired state, and chooses the appropriate feedforward trajectory, the appropriate feedback gains, or both. If the feedback component is presumed to reside at lower levels of the CNS, e.g., the spinal cord, this model is then compatible with a hierarchical concept of motor control. If the effect of the feedforward component is presumed small, and state feedback is the main component of the response, then control selection effectively chooses the appropriate gain matrix, in a scheme similar to the popular control engineering technique of gain-scheduling [33].

E. Compatibility with Constraints and Feasible Accelerations

Constraints placed on the system by the mechanics of the human body and the musculoskeletal configuration interact heavily to influence the control choices available. Constraints include keeping the knees straight (as has been experimentally observed in human responses to backward perturbations of the support surface which pitch the body forward), keeping the feet flat on the ground (as subjects are instructed to do), as well as limits on maximal muscle forces. The characterization of these constraints is summarized briefly here (see [19], [21]).

The feasible acceleration set (FAS) is the set of all joint angular accelerations (assembled in vector $\ddot{\theta}$) that can be produced by any combination of feasible muscle activations (that is, with normalized activation levels within the range $0 \leq a_i \leq 1$ for $i = 1, 2, \ldots m$ muscles). The FAS can be found from the mapping

$$\ddot{\theta} = La + g. \tag{1}$$

This mapping (see Fig. 2) is derived from the equations of motion (where L is a linear mapping and g represents a constant term), musculoskeletal geometry, and muscle properties, assuming that muscles are shortening slowly and excitation-contraction dynamics are fast in relation to the movement [35]. For a sagittal plane model that allows ankle, knee, and hip motion, this set is a polyhedron in joint angular acceleration space (Fig. 3(a)).

Acceleration vectors reaching the boundary of the FAS require at least one muscle to be fully activated. The FAS can therefore be used as a measure of the amount of acceleration that can be achieved in any direction in ankle-knee-hip acceleration space for a given amount of *neural effort*, defined as $\|a\|_\infty$, the maximum of the muscle activations a. This is

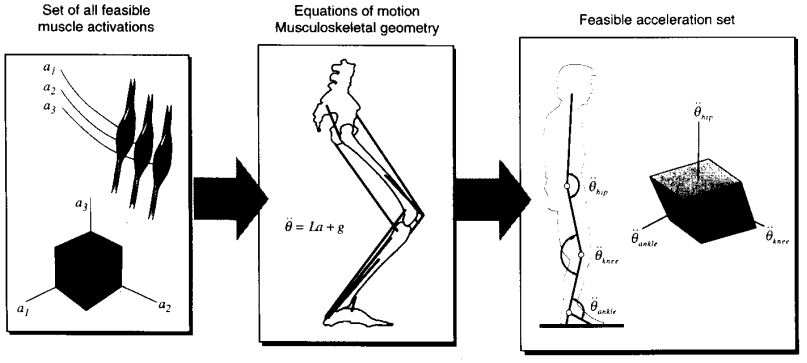

Fig. 2. Generation of feasible acceleration sets (FAS) is performed by characterizing the set of all feasible normalized muscle activations, which are confined to a hypercube, followed by generation of a mapping describing the effects of musculoskeletal geometry and equations of motion, into the set of all feasible joint angular accelerations. Result is a polytope in n-dimensional space, where n is the number of degrees of freedom studied. In this example, the feasible activations of three muscles are confined to a cube. These activations are mapped into feasible accelerations constrained within a 3-D polyhedron.

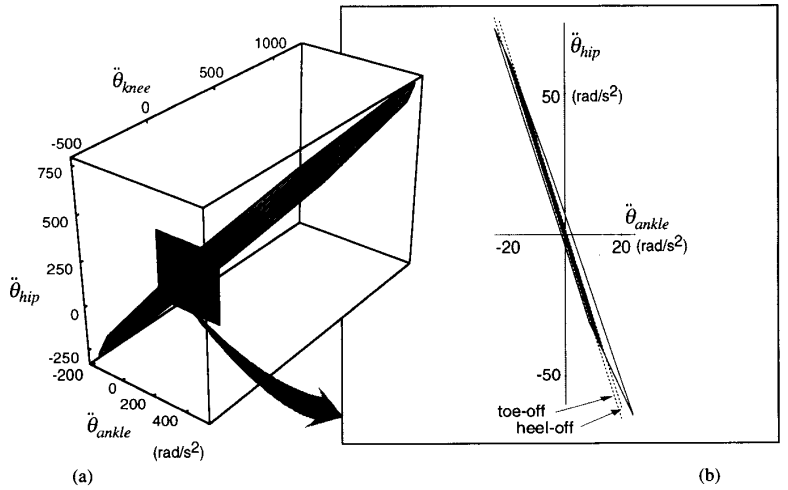

Fig. 3. (a) Ankle-knee-hip feasible acceleration set describes all combinations of joint angular accelerations achievable given any set of muscle activations. Enforcement of control constraint to keep knees straight, as human subjects do in natural response to backwards platform movement, is modeled by intersecting FAS with the plane corresponding to zero knee motion. (b) Enlargement of resulting ankle-hip FAS (keeping knees straight), showing effect of additional control constraints on avoiding lifting of toes and heels off the ground (dark region).

a convenient method for describing the aggregate cost of a given combination of joint angular accelerations, taking into account not only the joint torques needed (as with the model of [9]), but also the muscle forces needed to achieve those torques. Note that, given the assumptions above, neural effort is equivalent to the amount of muscle force (normalized to maximum possible force).

Visualization of the FAS aids in understanding constraints relevant to human posture. Researchers have reported that the knees are kept relatively straight while countering disturbances that pitch the body forward [26], [3]. The reasons behind and effects of this behavior (see [20]) are not discussed here, but this constraint must nevertheless be modeled. This modeling of constrained knee motion is accomplished by intersecting the polyhedron with the plane corresponding to $\ddot{\theta}_{\text{knee}} = 0$. The resulting polygon represents the set of all feasible accelerations of the ankles and hips when keeping the knees straight (see Fig. 3(b)) [20].

The length of the foot (or the support surface underneath the foot) dictates limits both to stable body configurations and to angular accelerations that can be achieved without lifting either the toes or heels off the ground, a common experimental requirement [26]. The body position constraints characterize the horizontal location of the body center of mass, which must remain over the base of support for stable stance. The linearized equation is of the form

$$c_{\text{cm0}} \leq c_{\text{cm}}^T \theta \leq c_{\text{cm1}} \tag{2}$$

where θ is the vector of joint angles. The desire to keep the feet flat on the ground is similarly written as the constraints

$$c_{\text{heel}}^T \ddot{\theta} \leq c_{\text{heel0}} \tag{3a}$$

$$c_{\text{toe}}^T \ddot{\theta} \leq c_{\text{toe0}}. \tag{3b}$$

When displayed in ankle-hip space (that is, with knees kept fixed), the constraint boundaries are approximately aligned

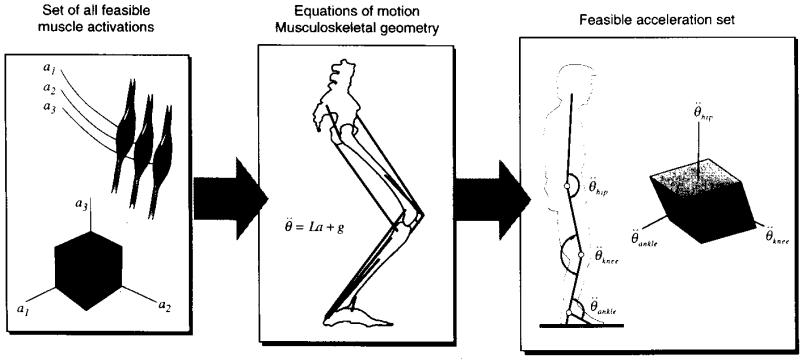

Fig. 2. Generation of feasible acceleration sets (FAS) is performed by characterizing the set of all feasible normalized muscle activations, which are confined to a hypercube, followed by generation of a mapping describing the effects of musculoskeletal geometry and equations of motion, into the set of all feasible joint angular accelerations. Result is a polytope in n-dimensional space, where n is the number of degrees of freedom studied. In this example, the feasible activations of three muscles are confined to a cube. These activations are mapped into feasible accelerations constrained within a 3-D polyhedron.

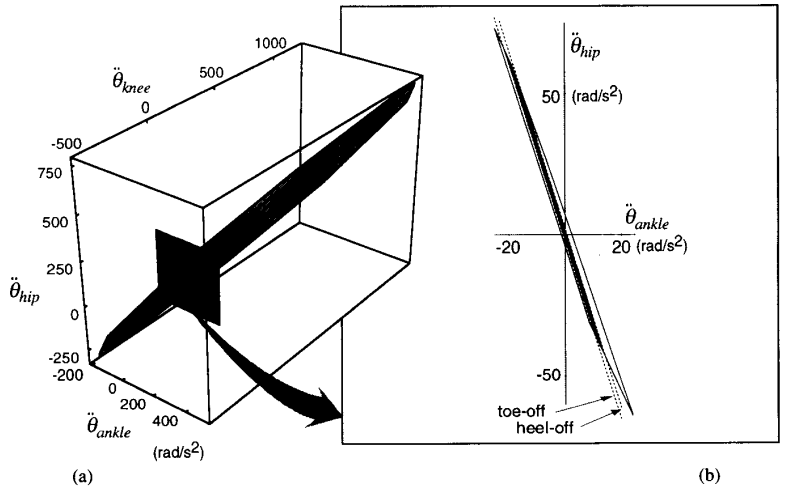

Fig. 3. (a) Ankle-knee-hip feasible acceleration set describes all combinations of joint angular accelerations achievable given any set of muscle activations. Enforcement of control constraint to keep knees straight, as human subjects do in natural response to backwards platform movement, is modeled by intersecting FAS with the plane corresponding to zero knee motion. (b) Enlargement of resulting ankle-hip FAS (keeping knees straight), showing effect of additional control constraints on avoiding lifting of toes and heels off the ground (dark region).

a convenient method for describing the aggregate cost of a given combination of joint angular accelerations, taking into account not only the joint torques needed (as with the model of [9]), but also the muscle forces needed to achieve those torques. Note that, given the assumptions above, neural effort is equivalent to the amount of muscle force (normalized to maximum possible force).

Visualization of the FAS aids in understanding constraints relevant to human posture. Researchers have reported that the knees are kept relatively straight while countering disturbances that pitch the body forward [26], [3]. The reasons behind and effects of this behavior (see [20]) are not discussed here, but this constraint must nevertheless be modeled. This modeling of constrained knee motion is accomplished by intersecting the polyhedron with the plane corresponding to $\ddot{\theta}_{\text{knee}} = 0$. The resulting polygon represents the set of all feasible accelerations of the ankles and hips when keeping the knees straight (see Fig. 3(b)) [20].

The length of the foot (or the support surface underneath the foot) dictates limits both to stable body configurations and to angular accelerations that can be achieved without lifting either the toes or heels off the ground, a common experimental requirement [26]. The body position constraints characterize the horizontal location of the body center of mass, which must remain over the base of support for stable stance. The linearized equation is of the form

$$c_{\text{cm0}} \leq c_{\text{cm}}^T \theta \leq c_{\text{cm1}} \tag{2}$$

where θ is the vector of joint angles. The desire to keep the feet flat on the ground is similarly written as the constraints

$$c_{\text{heel}}^T \ddot{\theta} \leq c_{\text{heel0}} \tag{3a}$$

$$c_{\text{toe}}^T \ddot{\theta} \leq c_{\text{toe0}}. \tag{3b}$$

When displayed in ankle-hip space (that is, with knees kept fixed), the constraint boundaries are approximately aligned

III. Mathematical Description of Model

The LQG regulator is a state feedback that minimizes an objective of the form

$$J = \int_0^\infty E\left[x^T Q x + u^T R u\right]\, dt, \tag{6}$$

where Q and R are weighting matrices for states x and controls u, respectively [6]. The system dynamics are described by a set of time-invariant first-order linear equations of the form

$$\dot{x} = Ax + Bu + w \tag{7a}$$

$$y = Cx + Du + v \tag{7b}$$

where y is a vector of output or sensor states, and system matrices A, B, C, and D include both the mechanics of the body and the dynamics of sensors, depending on the desired complexity of the model. Process noise w and sensor noise v are modeled as Gaussian white-noise random processes with power spectral density matrices W and V, respectively. Though the estimator is an integral part of the model, this paper does not deal with specific effects of noise, and W and V are left unmodeled. From the certainty-equivalence principle [6], the controller can be designed independently of the state estimator implementation.

A. State Equations for Rigid Body Mechanics

The first step in developing equations for rigid body mechanics is determination of state realization and dimension. Many realizations will produce the same transfer function matrix and input-output behavior. It is difficult, if not impossible, to determine the actual physiological states employed by the CNS because of their quantity and relative inaccessibility [29]. The particular state realization selected, while affecting some measures of relative controllability and observability, such as the grammian functions [17], is of little importance here. For modeling the mechanics of human standing in conditions in which the knees remain relatively straight, it is reasonable to choose a reduced-order four-state system, corresponding to the two-joint system utilized by others [9], [3]. Its realization is arbitrarily based on joint angles (ankle and hip), as these are commonly measured in experiments.

Using the feasible acceleration set for upright standing with the knees kept straight (Fig. 3(b)), it is possible to decouple the model, so that controls are described in strategy space rather than torque space (see above). With the reduced-order state and controls defined as

$$x_r \equiv \begin{bmatrix} \theta_{\text{ank}} \\ \theta_{\text{hip}} \\ \dot{\theta}_{\text{ank}} \\ \dot{\theta}_{\text{hip}} \end{bmatrix}, \quad u_r \equiv \begin{bmatrix} u_{\text{ank}} \\ u_{\text{hip}} \end{bmatrix}$$

and system matrices

$$A_r \equiv \begin{bmatrix} 0 & 0 & 1 & 0 \\ 0 & 0 & 0 & 1 \\ 0 & 0 & 0 & 0 \\ 0 & 0 & 0 & 0 \end{bmatrix}, \quad B_r \equiv \begin{bmatrix} 0 & 0 \\ 0 & 0 \\ 1 & -7.7 \\ 0 & 24.5 \end{bmatrix}$$

this double-integrator model is in the form of (7)

$$\dot{x}_r = A_r x_r + B_r u_r. \tag{8}$$

Note that values for B_r are taken from (4), leaving out the terms for knee acceleration.

The feedback K_r for this decoupled system, found using Q and R as described in [33], must return a specific combination of ankle and hip strategies u_r given the states x_r

$$u_r = -K_r x_r \tag{9}$$

where $K_r \in \Re^{2\times 4}$. The desired joint angular accelerations $\ddot{\theta}_d$ can be found by

$$\ddot{\theta}_d = B_{r2} \cdot u_r \tag{10}$$

where B_{r2} is the lower half of B_r.

The model of (8) maintains compatibility with other linear models (e.g., [3]), such as

$$\dot{x}_m = A_m x_m + B_m u_m \tag{11}$$

where $A_m \in \Re^{6\times 6}$, $B_m \in \Re^{6\times 3}$ are derived from the linearized equations of motion, and the states and controls are

$$x_m \equiv \begin{bmatrix} \theta_{\text{ank}} \\ \theta_{\text{kne}} \\ \theta_{\text{hip}} \\ \dot{\theta}_{\text{ank}} \\ \dot{\theta}_{\text{kne}} \\ \dot{\theta}_{\text{hip}} \end{bmatrix}, \quad u_m \equiv \begin{bmatrix} T_{\text{ank}} \\ T_{\text{kne}} \\ T_{\text{hip}} \end{bmatrix}.$$

Note that constraining *motion* of the knee as in this study does not imply absence of *torque* about the knee, which is necessary to keep the knee straight. Conversion to the three-joint, torque-based model (11) is accomplished as follows. First, the matrices A_r, B_r, and K_r must be expanded to correspond to x_m, u_m, including the knee (though it is kept motionless). Written compactly, the result is

$$A_r^{(3)} \equiv \begin{bmatrix} 0 & I^{3\times 3} \\ 0 & 0 \end{bmatrix}, \quad B_r^{(3)} \equiv \begin{bmatrix} 0 \\ b \end{bmatrix},$$

$$K_r^{(3)} \equiv \begin{bmatrix} K_{r11} & 0 & K_{r12} & K_{r13} & 0 & K_{r14} \\ K_{r21} & 0 & K_{r22} & K_{r23} & 0 & K_{r24} \end{bmatrix}.$$

The desired accelerations θ_d can be expanded to $\theta_d^{(3)} \in \Re^3$ for ankle, knee, and hip joints, leaving the knee acceleration zero. Then, using (4),

$$\ddot{\theta}_d^{(3)} = b \cdot u_r \tag{12}$$

similar to (10). Joint torques necessary to execute these desired accelerations are found from

$$u_m = B_{m2}^{-1}(\ddot{\theta}_d^{(3)} - A_{m2} x_m) \tag{13}$$

where A_{m2} and B_{m2} are taken from the lower half of (11). This relation can be used in solving (11) to compute the feedforward components of the ankle, knee, and hip joint torques necessary to execute the selected control strategies, keeping the knee straight. (The resulting knee torque is presumed to be supplied by active muscle force or by constraints on knee motion.) However, this model does not include a direct

feedback of knee angle, which would be necessary in practice, but which is assumed to be relatively small in magnitude if the feedforward component is accurate.

Inclusion of sensory dynamics is described in Appendix A.

IV. Formulation and Testing of Objectives

With $x = x_r$ and $u = u_r$ (assuming no knee motion), the weighting matrices R and Q of (6) can be chosen so as to penalize excessive exertion of control effort (or neural effort as defined in Section II) and undesired excursions of the state from stable upright posture. However, R and Q contain a total of 13 independent entries (of 4 entries in R and 16 entries in Q, due to symmetry), which prove difficult to specify based on either theoretical considerations or experimental data. Simplification of the objective function is accomplished first by reducing the number of free entries, and then parametrizing R and Q so that physically meaningful objectives subject to constraints may be implemented. For example, Q is parametrized by variables corresponding to the size of perturbation and the relative amount of hip and ankle strategies used, which are related to the constraints to keep the feet flat on the ground. The controller is to evaluate the state after a perturbation and then set then gain matrix parameters. Preliminary experimental data are used to provide rough estimates of equivalent parameter values used by the CNS.

A. Formulation of Weighting Matrix on Controls

With state feedback, the closed-loop system poles can be placed arbitrarily; matrix R models the effort associated with movement of these poles. If R is chosen to be the identity matrix,

$$R = \begin{bmatrix} 1 & 0 \\ 0 & 1 \end{bmatrix}; \tag{14}$$

it will have the effect of weighting the relative costs of the ankle and hip strategies equally. Equation (4) defines the basis b, describing accelerations resulting from each strategy, so that for equal neural effort, the hip strategy will produce accelerations of larger magnitude than the ankle strategy. The cost of executing the ankle or hip strategies is thereby factored into R. Fig. 4(a) illustrates this cost in joint angular acceleration space. Alterations to (14) can also be used to change the relative weightings of the two strategies.

B. Formulation of Weighting Matrix on States

The Q matrix in (6) is chosen so as to simplify the equations governing the feedback gain matrix. First, Q is constrained to be positive definite (rather than the LQR requirement of positive semi-definiteness), so that there are no states other than the origin (upright stance) that minimize the objective on states. Second, Q is constrained to weight only joint angle deviations, excluding joint velocity weighting. Thus,

$$Q = \sigma^2 \begin{bmatrix} Q_{11} & 0 \\ 0 & 0 \end{bmatrix}, \tag{15}$$

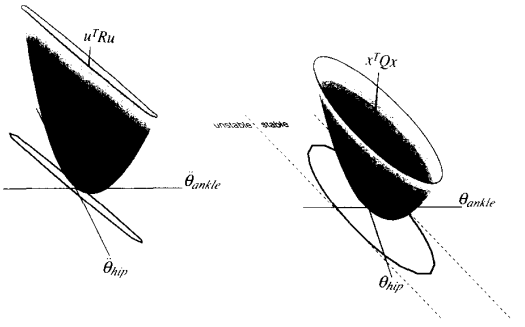

(a) (b)

Fig. 4. (a) Three-dimensional plot of cost function on the controls. In angular acceleration space, this function is modeled on the ankle-hip feasible acceleration set, shown in the ankle-hip acceleration plane (see Fig. 3). (b) Three-dimensional plot of cost function on the states. The [cm] objective, which models the desire to avoid horizontal excursion of the body center of mass beyond the support surface (unstable region), and the [up] objective, which models maintenance of upright stance, combine to form this surface. Note that minimum is at the origin, corresponding to upright position.

where σ is a scalar governing the relative weighting of Q and R (the maximum singular value of $Q_{11} \in \Re^{2\times 2}$ is constrained to be unity, i.e., $\bar{\sigma}(Q_{11}) = 1$). Such a formulation reduces the number of parameters needed to specify the objective to three (for positive definite Q). This reduction comes at the expense of control over the joint velocity weightings and hence, the relative damping of the system. Instead, the inherent properties of the LQR-designed controller are assumed to provide a well-damped control that adequately approximates both the desired and actual behavior.

C. Selection of State Objectives

Although Q of (15) could be chosen by trial-and-error selection of each entry, the specification of the state objectives is vastly simplified by choosing Q so that certain physical quantities relevant to posture are regulated. These choices reduce the solution space to be searched and reflect the constraints imposed by the biomechanics of the system. The control responses dictated by the regulation of each physical quantity can be examined, providing clues as to which combinations produce behavior most similar to that observed experimentally. It is proposed that relevant quantities include center-of-mass position, upright body position, and head position.

It is assumed that the body is subject to constraints in ankle-hip position space—that is, the horizontal location of the center of mass should be regulated to remain within the base of support, as in (2). This constraint can be modeled as a penalty function of the form $\left(c_{\text{cm}}^T\theta\right)^2$, where $c_{\text{cm}} \equiv [-0.98 - 0.23]^T$ (see [19]), so that larger costs are associated with progressively less balanced configurations. This center of mass stabilization objective, [cm], is presumed to be a large factor in the state cost function.

Because the CNS controls the body not only for balance but for maintenance of upright stance, another factor in the

TABLE I
COST FUNCTIONS AND Q MATRICES FOR VARIOUS OBJECTIVE FUNCTIONS

Cost function	Q matrix	Objective
$(c_{cm}^T\theta)^2$	$Q_{cm}=\begin{bmatrix} c_{cm}c_{cm}^T & 0 \\ 0 & 0 \end{bmatrix}$	[cm]
$\theta^T\theta$	$Q_{up}=\begin{bmatrix} I^{2\times 2} & 0 \\ 0 & 0 \end{bmatrix}$	[up]
$(c_{hd}^T\theta)^2$	$Q_{hd}=\begin{bmatrix} c_{hd}c_{hd}^T & 0 \\ 0 & 0 \end{bmatrix}$	[hd]

cost function should be regulation of body position. This hypothetical objective, [up], is of the form $\theta^T\theta$, so as to penalize all positions away from upright stance.

The objective can also be based on the proposed desire to regulate head position so as to provide a stable platform for the eyes [2]. Head angle, which is not included in the state vector x_m, can be regulated with respect to the horizontal regardless of movement of the body, so that the stable platform can be maintained without requiring alterations to objectives on x_m. However, due to the existence of noise and thresholds in the controller, deviations in head angle can be expected to increase with increased body motion. To minimize this uncertainty, the body should provide a stable platform for the head [hd] by keeping the trunk vertical. As the trunk angle is derived from the sum of the ankle and hip angles, a cost function $(c_{\rm hd}^T\theta)^2$, where $c_{\rm hd} \equiv [1\ 1]^T$, penalizes movement of the trunk away from vertical.

The sample cost functions for hypothetical objective [up], [cm], and [hd] are summarized in Table I. It is expected that a cost function emulating human behavior would consist of a combination of one or more of these costs. To gain insight into the effects of each of these objectives, it is possible to plot their resultant trajectories to gauge how various combinations would perform. Ankle-hip trajectories for the [cm], [up], and [hd] objectives are plotted in Fig. 5. The [cm] and [hd] objectives were augmented with small proportions of [up] to ensure positive definiteness. Note that [cm] produces curved trajectories similar to the hip strategy discussed in [26], while the [up] objective tends to attract the trajectory to the ankle axis. The [hd] objective produces curved trajectories which are opposite in direction to those from [cm]. This indicates that combinations of [cm] and [up] might produce trajectories similar to the ankle strategy. The form of such a combined objective is shown in Fig. 4(b).

D. Parametrization of Objective

Final determination of Q involves selection of parameters to specify combinations of the objectives discussed above. As seen in (15), Q is specified by three independent entries, and therefore three free parameters. With proper formulation, the objective parameters may be interpreted in a number of physically meaningful ways. As formulated here, one parameter is used to select the type of response, another selects the speed or gain of the response, and one is left unused.

Using the proposed combination of [cm] and [up] objectives as a framework, it is natural to choose a parameter μ to govern

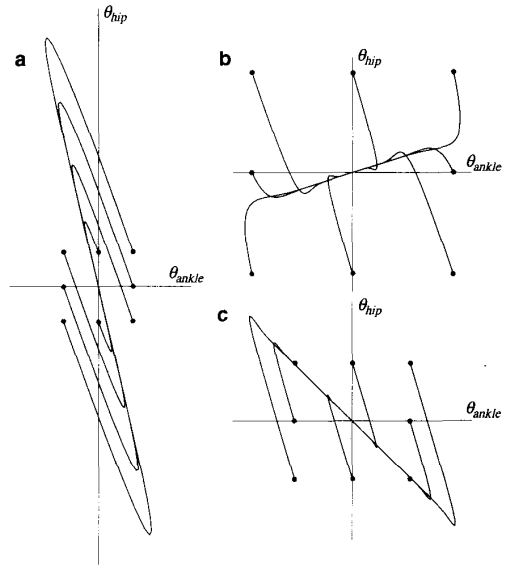

Fig. 5. Ankle-hip trajectories for various objectives. (a) [cm] objective (regulation of body center of mass) results in counterclockwise curved trajectories. (b) [up] objective (regulation of upright stance) controls hip angle quickly, followed by motion about the ankles toward upright. (c) [hd] objective (minimization of excessive head motion needed to maintain level gaze) produces curved trajectories opposite in direction to those of [cm].

the proportion of [cm] and [up] in Q. Another parameter σ can be used to regulate the overall magnitude of Q relative to R, leaving one additional parameter, ϕ, which is arbitrarily defined as the rotation of the [cm] and [up] components in the ankle-hip plane (about the vertical axis in Fig. 4(b)). This parameter is left at $\phi = 0$ in this formulation. The resulting objective can then be written as

$$Q = \sigma^2 \frac{\mu Q_{\rm cm} + (1-\mu)Q_{\rm up}}{\overline{\sigma}(\mu Q_{\rm cm} + (1-\mu)Q_{\rm up})}. \tag{16}$$

Ensuring that $0 \le \mu < 1$ and $\sigma > 0$ guarantees that Q is positive definite. Normalizing by the maximum singular value of the numerator, $\overline{\sigma}(\bullet)$, guarantees that variation of μ does not interfere with the magnitude-scaling properties of σ. Thus, the entire response properties of the system are specified by the two parameters μ and σ (leaving the third unused).

There are several functions that can be ascribed to μ and σ so as to aid understanding. The proportion of [cm] and [up] as governed by μ is equivalent to specifying the ratio of hip and ankle strategies. The parameter σ is subject to a number of interpretations relating to the speed or gain of the response. For example, magnitude-scaling of Q with σ also parametrizes the gain matrix K_r. As discussed in Appendix A, the relation is

$$K_r = [\sigma K_1 \ \sqrt{\sigma} K_2] \tag{17}$$

where $K_1, K_2 \in \Re^{2\times 2}$ are nominal matrices found by solving the Riccati equation with $\sigma = 1$.

The relation between σ and the center of mass acceleration is also simplified. If the effect of the disturbance can be modeled as a perturbation on the initial values of θ while having little effect on $\dot{\theta}$ (because the support surface is started and stopped quickly), that is,

$$x_0 \approx \begin{bmatrix} \theta_0 \\ 0 \end{bmatrix},$$

then the linearized expression for horizontal acceleration of the center of mass, $\ddot{z}_{\rm cm}$, is a linear function of joint angular accelerations [20],

$$\ddot{z}_{\rm cm} = c_{\rm cm}^T \ddot{\theta} \tag{18}$$

and can be related to x_r using (9) and (10), to form the relation

$$\ddot{z}_{\rm cm} = c_{\rm cm}^T B_{r2} K_r x_r. \tag{19}$$

For a minimum-phase system such as this, the maximum value of $|\ddot{z}_{\rm cm}|$ occurs at initial time and is found by substituting initial conditions into (19). Also substituting (17),

$$\ddot{z}_{|\max|} = \max|\ddot{z}_{\rm cm}| = \left|\sigma c_{\rm cm}^T B_{r2} K_1 \theta_0\right| \tag{20}$$

where $\theta_0 \equiv [\theta_{\rm ank}\ \theta_{\rm hip}]^T$ at initial time, so that there is a linear relationship between σ and $\ddot{z}_{|\max|}$. This proportionality implies that and can be used interchangeably as parameters.

The constraints (3) for keeping the feet flat on the ground are similar in form to (18), implying that σ is also linearly related to heel- and toe-off conditions. Thus, the parameter σ has a direct relationship to the feedback K_r, the maximum center of mass acceleration, and heel- or toe-off. Depending on the application, σ can then be interpreted alternatively as a measure of the relative cost of state deviations, the speed of the response, the gain of the feedback, the amount by which we are willing to move the system poles, or the danger of lifting the toes or heels off the ground.

The actual values for μ and σ are chosen by the control selection center (Fig. 1(b)) based on the size of disturbance. It is expected that the penalty [cm] is of greater importance when responding to larger perturbations, when the constraint of keeping the center of mass within the base of support is likely to become active. As perturbations increase, the acceleration of the body required to offset the perturbation will also increase. The control selection center is therefore expected to increase both μ and σ as pertubations increase in size. The model implements the selected control for the duration of the response.

E. Comparison with Experimental Observations

The model utilizing objective function (16) was compared with natural human responses, where subjects were released from various initial positions and allowed to return naturally to upright stance. Ankle-hip trajectories were found to exhibit a curved shape similar to those described in [26]. Thus, the simple LQR objective scheme, in conjunction with body dynamics, was sufficient to reproduce major characteristics of human responses without need for more complex objectives involving switching between strategies and minimizing the number of muscles used [26].

Measured ankle and hip trajectories were used to find rough estimates of parameter values and to test predictions on how these parameters varied with initial conditions. Use of initial conditions rather than platform movement as disturbance was used to simplify the model validation procedure.

To compare with experimental results, objective function parameters were chosen to best match experimental trajectories. The parameter σ was used to scale the temporal response to match natural responses, while μ was adjusted to match ankle and hip angle trajectories and model the enforcement of constraints that become active as perturbations become larger or initial conditions approach the position constraints of (2). Simulations with these parameter values show that the model (8), using objectives [cm] and [up], minimizing neural effort, produces curved trajectories similar to those described in [26], as shown in Fig. 6 (this is only a subspace of the full 4-D state space, which is difficult to illustrate). For larger disturbances, values of $\mu = 0.997$ produce reasonable matches, similar to the kinematics of the hip strategy; for small disturbances, values of $\mu = 0.980$ produce trajectories similar to the kinematics of the ankle strategy. (Note that the small range of values for μ is an artifact of the parametrization, and is not indicative of a sensitivity problem in the model or the CNS.)

For a given initial condition, $\ddot{z}_{|\max|}$ can linearly parametrize σ using (20). Elements of feedback gain matrices K_r are plotted versus varying values of $\ddot{z}_{|\max|}$ (and hence σ) and μ in Fig. 7. Note that the feedback gain increases with $\ddot{z}_{|\max|}$, verifying that control effort increases in magnitude with the speed of the response required to offset a disturbance. As μ decreases, lowering the proportion of [cm] in the objective, the relative proportion of ankle strategy is increased. Large values of μ produce gains utilizing higher proportions of the hip strategy. This indicates that for a given $\ddot{z}_{|\max|}$, ankle strategy movements tend to require more control effort than hip strategy movements.

Fig. 8 illustrates the performance of the controller for varying values of $\ddot{z}_{|\max|}$ and μ. Note that susceptibility to lifting of the heels off the ground, $c_{\rm heel}^T \ddot{\theta}$, increases as $\ddot{z}_{|\max|}$ increases and as μ decreases (Fig. 8(a)). Thus, a secondary effect of the [cm] objective is that the constraints (3) are not active for large values of μ, so that the feet are automatically kept flat on the ground. Fig. 8(b) shows that settling times (time for response to return within 10% of zero) are fairly invariant with μ; the choice of objective, and therefore strategy, has little bearing on response time.

An important consideration in a biological system is that the controller must be stable even with substantial transmission delays. The maximal time delay tolerable before a system becomes unstable may be estimated by determining the phase margin of the system and dividing by the cross-over frequency to find the largest tolerable pure lag. Maximum tolerable time delays for varying values of $\ddot{z}_{|\max|}$ and μ, are shown in Fig. 8(c). Note that, except for slow responses (small values of $\ddot{z}_{|\max|}$), there is little variance in robustness to time delays with respect to μ. For very small disturbances that can be stabilized with small $\ddot{z}_{|\max|}$, larger values of μ, corresponding to controls similar to the hip strategy, are more robust with respect to time delays.

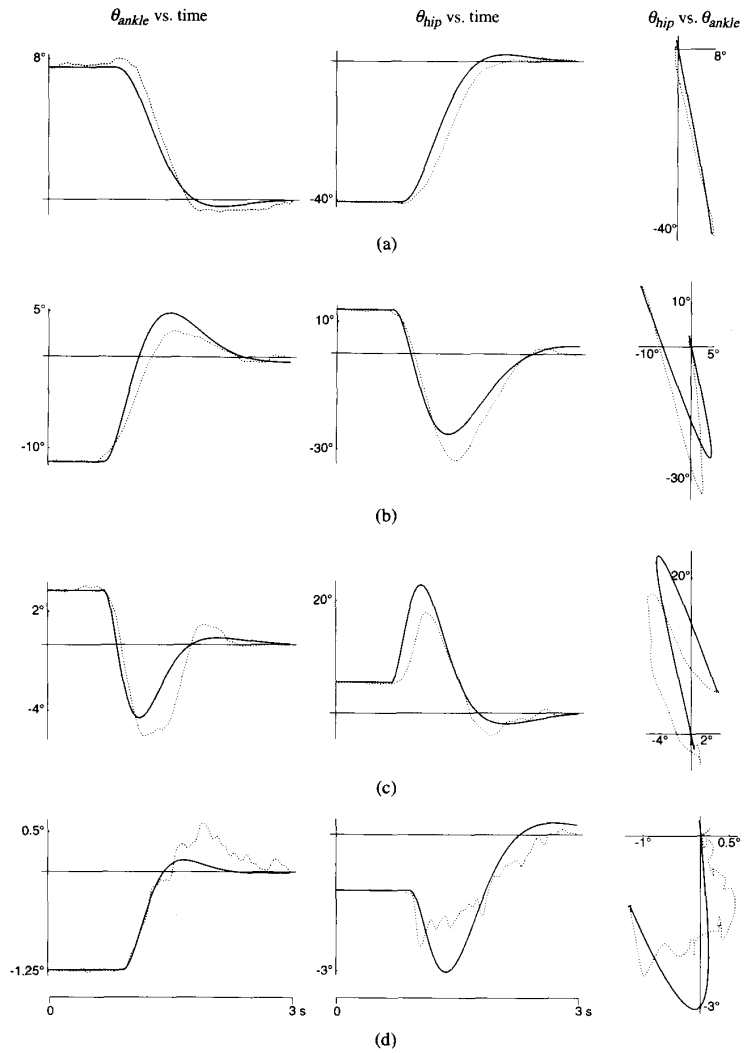

Fig. 6. Comparison of experimental data (dotted lines) with computed simulations (solid lines). Data are from a typical subject released from various initial positions, returning to upright stance. Shown are ankle angle θ_{ank} versus time, hip angle θ_{hip} versus time, and θ_{hip} versus θ_{ank}. (a) Starting with ankle extended, hip flexed. $\sigma = 1.4$, $\mu = 0.997$. (b) Starting with ankle flexed, hip extended. $\sigma = 2.4$, $\mu = 0.997$. (c) Starting with ankle flexed, hip extended. $\sigma = 1.6$, $\mu = 0.990$. (d) Starting with ankle flexed, hip flexed. $\sigma = 0.6$, $\mu = 0.980$.

V. Discussion

A. Modeling Deficiencies

Many of the differences between experimental and simulated trajectories can be attributed to simplifications in the modeling and formulation of the objective. Errors in prediction will arise due to flexibility within the human body segments, and particularly, nonnegligible knee motion. In particular, inclusion of knee motion in the model is believed to increase fidelity to experimental results, though at the cost of increased complexity. The additional degree of freedom increases the dimension of the state vector, and may require one or more additional parameters to form the cost function.

Knee motion can also be presumed to be dependent on the direction of the disturbance. A person falling forward over the toes might be expected to bend forward over the hips while rotating backwards about the ankles slightly (thereby moving the center of mass backwards), keeping the knees straight and fully extended. A person falling backward might be constrained from reversing this response due to limitations on hip extension, and may rely on flexing the knees to move the center of mass horizontally. Thus, knee motion, if modeled, must be made dependent on the direction of the disturbance and constraints on hyperextension. This nonlinearity could be accounted for by using the gain-selector with two linear models—one for each direction of perturbation.

The LQG controller produces an optimal return trajectory that is a function of the states. To study platform perturbations, it is necessary to provide reasonable estimates of initial conditions on the states which are used to compute the return trajectory. Because the platform imparts changed velocities,

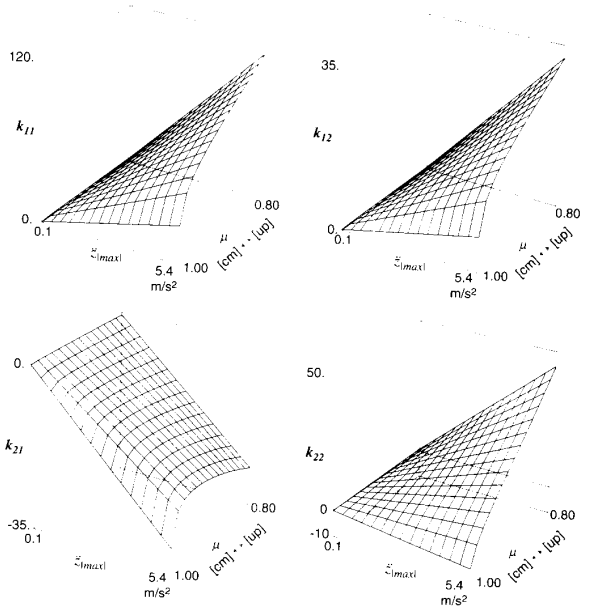

Fig. 7. Gain matrix elements K_{ij} versus $\ddot{z}_{|\max|}$ (maximum center of mass acceleration) and μ. First row is gain feeding back to ankle strategy, and second row feeds back to hip strategy. First column is feedback from ankle position. Second column is feedback from hip position. Note that gain increases, indicating larger control effort, as the speed increases. Decrease of μ causes greater proportion of ankle strategy. Increase in μ causes greater proportion of hip strategy.

as well as positions to the system, the initial conditions on positions (used here to model standing up after release from nonerect stance) must be augmented with velocity information. Alternatively, perturbations may be modeled as exogenous force or acceleration inputs, which would require additional degrees of freedom for support surface movement.

The model here also relies on feasible acceleration sets to model the cost of activating muscles. Other possible cost functions utilizing metabolic or mechanical energy expenditure (see, e.g., [31]) are difficult to implement using quadratic functions. Minimization of neural effort serves as an adequate cost in that it penalizes increased activation of muscles and integrates this cost over the entire trajectory. It does not account for the velocity of movement, whether the muscles are lengthening or contracting, or whether muscles are co-contracting.

Both regulator and estimator portions of the LQG controller are implemented using steady-state feedback gains. Steady-state gains are appropriate for the middle portion of a long trajectory. Linear quadratic regulators are expected to use time-varying gains near the end of a trajectory, when terminal objectives, which are not part of the objective in the current model, may have precedence. Similarly, state estimators are expected to use time-varying gains near the beginning of a trajectory, when initial conditions on the state estimate may have precedence over the computed values [6]. The use of steady-state gains greatly simplifies computation and simulation, at the expense of accuracy at the initial and final portions of the trajectory. This accuracy could be improved by implementing a terminal objective and time-varying gains for a finite-time task.

B. Analysis of Time Delay Robustness

The optimal control model appears to be useful for testing motor control hypotheses, despite the deficiencies outlined above. For example, it is possible to examine the robustness of the ankle and hip strategies to transmission delays. (Note that robustness of an LQG controller can be recovered using loop transfer recovery [8].) Analysis (Fig. 8(b)) shows that controllers utilizing the hip strategy (larger values of μ) can tolerate greater time latencies before going unstable than those utilizing the ankle strategy (smaller values of μ). These findings are in contrast with those of [24], in which time constants for the inverted pendula corresponding to the two strategies were computed and compared. It was concluded in [24] that because a response must be produced within a quarter-period of the movement, the slower ankle strategy is more tolerant to time latencies. The difference in results can be explained by analyzing the feedback control system. State feedback can be used to move system poles (and hence, time constants) to arbitrary locations. This movement of poles is limited by the cost of the control large feedback gains are necessary to move poles far from their open-loop locations. While the hip strategy is naturally faster than the ankle strategy as shown in [20] and [24], it also requires smaller feedback gains to achieve a given speed of response.

This analysis shows that when the controllers are analyzed with respect to center of mass acceleration ($\ddot{z}_{|\max|}$), a given disturbance can be countered either by a hip strategy ($\mu = 0.997$) with low gain, or an ankle strategy ($\mu = 0.980$) with higher gain. Because the magnitude of feedback gain, rather than the strategy used, is the primary determinant of time delay robustness, there is little or no advantage to the ankle strategy—a hip strategy can stabilize the body just as quickly, but with lower gain. As a result, the hip strategy can actually tolerate longer transmission delays while maintaining stability.

C. Interpretation of Objective Function

Once a cost function has been shown to produce a reasonable approximation of natural behavior, it is natural to interpret the objective being achieved. For example, the controller introduced here appears to regulate center-of-mass position above the support surface with an additional objective of maintaining upright stance (the [cm] and [up] objectives). The gain-selecting model that matches human behavior would choose slow movements (small values for σ) mostly of the ankle strategy ($\mu \approx 1.00$) for small disturbances. As disturbances to posture become larger, the gain-selector would choose progressively faster responses (larger values for σ) using the hip strategy ($\mu \approx 0.98$) to avoid lifting the feet off the ground. The resulting controller behaves functionally like the CNS, choosing the ankle strategy for smaller disturbances, switching to the hip strategy for larger disturbances.

It is quite possible that such a cost function results in a controller that approximates natural behavior well. It is also quite possible that there exist neural circuits that compute

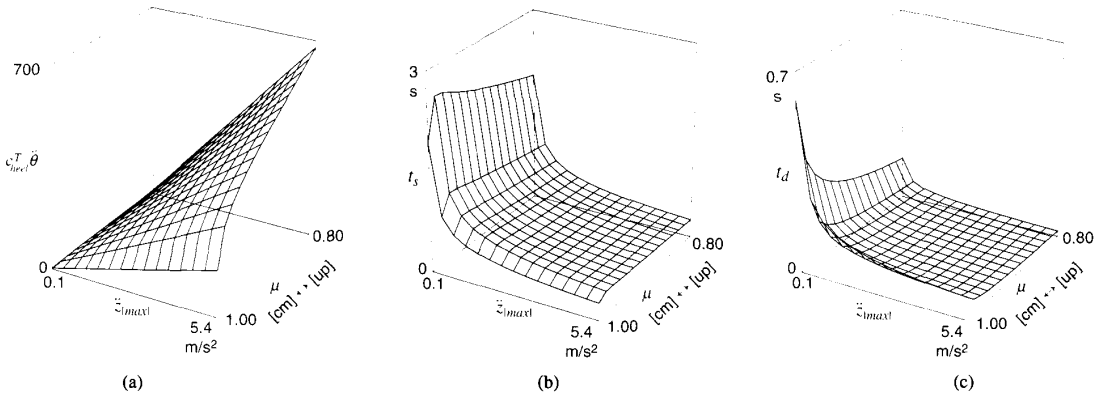

Fig. 8. Performance of system versus $\ddot{z}_{|\max|}$ and μ. (a) Susceptibility to lift-off of the heels, $c_{\text{heel}}^T\ddot{\theta}$, increases with speed of movement and use of ankle strategy (low μ). (b) Settling time from disturbance remains approximately the same for both ankle and hip strategies ([cm] and [up] objectives). Slower movements have slower settling times. (c) Maximum tolerable time delay, calculated from phase margin of stabilized control system. Note that neither strategy has a large advantage, but for extremely slow movements, [cm] objective appears most robust.

such a cost function. However, it is fruitless to attach an interpretation (e.g., that the CNS desires to regulate position of the center of mass) to the cost function, because there are many other possible interpretations that produce the same results. For example, a controller could be implemented using a combination of [cm] and [hd] objectives, and with the appropriate choice of rotation ϕ, could exactly duplicate the cost function (16). Such a controller was rejected based on intuitive interpretations of ankle-hip trajectories in Fig. 5 and to avoid use of additional parameter ϕ. But none of the above results provide any evidence for rejecting [hd] as a component of the actual objective used by humans. The use of [cm] and [up] objectives in (15) was based primarily on the desire to reduce the size of the parameter space to be searched. Thus, while intuition aids in formation of hypotheses concerning objectives, and some objectives may be deemed unlikely after examination of the trajectories, the results have limited utility for interpretation.

Nevertheless, the *existence* of simple objectives is subject to interpretation. Evidence that the CNS flexibly adjusts controls based on mechanical constraints suggests that the CNS is not subject to certain neural constraints, as hypothesized in [26]. Rather, neural circuitry is programmed to stabilize the body subject to the varying effects of *external* mechanical constraints. More experimentation is required to accurately describe the objectives which describe how this flexibility is used.

More careful models of the cost function can produce predictions with greater fidelity to experimental results and superior predictive capability. The three degree-of-freedom quadratic cost function (15) could be replaced by more complex, possibly nonquadratic functions. However, the successful use of a simple quadratic function leaving velocity states unweighted indicates that only a few states are important to the CNS when adapting to changing situations.

Identification of significantly improved objective functions is ultimately limited by feasibility of the experiments, resolution of the data, and inter- and intrasubject variability. However, clever design of perturbations and conditions should aid in identification of much finer details of the objective than are discussed here. One use of these model mechanical systems is to identify which of the many variants of these experiments will provide the most powerful tests of competing hypotheses.

D. Compatibility Issues

Though more general nonlinear objective functions may improve fidelity, the LQG controller has a number of inherent advantages. First, the optimal return trajectory can be described as either a feedforward trajectory or a feedback control with constant gains in the steady state (see Section II). While there is considerable debate concerning the proportion of feedforward and feedback used by the CNS [21], [12], this model produces the same trajectories regardless of the proportion. This also makes the model compatible with feedback error-learning models [18], which incorporate both components. More complicated optimal control formulations generally produce only feedforward trajectories, without feedback gains which are of particular interest to neurophysiologists [10]. An exception is the technique of dynamic programming [33], which is highly susceptible to problems of dimensionality.

Second, LQG is a simple technique for design of full-state feedback systems compatible with those of [9], [3]. Such systems are also amenable to state space identification techniques, providing further avenues for experimental study.

The linearity of the controller is disadvantageous in that it requires a control selection center (Fig. 1) to estimate the size of the disturbance and whether constraints are active, and to select controller parameters (μ and σ) accordingly. However, others have proposed a hierarchical motor control scheme in which low-level regulation occurs in lower levels of the CNS (such as the spinal cord), with successively higher levels of feedback to portions of the brain [22]. The necessity of a control selection center is therefore compatible with such hierarchical control hypotheses.

The successful performance of the model does not, however, imply that the CNS functions as a linear quadratic regulator and estimator; nor is it proposed that there are

specific functions of the model (see Fig. 1) being performed in specific locations within the CNS. In fact, the separation of the regulator and the estimator in the model is only due to mathematical (the certainty-equivalence principle) and conceptual simplicity, and is not necessary in a controller implemented in neural circuitry. The only presumption is that for the specific operating conditions outlined here, the CNS achieves the same functionality as the LQG model, in that the system can stabilize against small perturbations, making efficient use of body biomechanics and (redundant) sensory information to produce the control.

The state estimator model of sensory output processing has significant advantages over the Sherringtonian concept of reflex loops from sensors to actuators [32]. The suggestion that the CNS utilizes an internal model of the body is compatible with data concerning responses to ambiguous sensory information, such as circularvection [5]. Incorporation of sensory information throughout the body to estimate states may also explain the enormous degree of divergence and convergence of neurons seen physiologically. The implication is that output from sensors is not used *directly* as a trigger or in multiplicative feedback to produce a response, as in the Sherringtonian view. Rather, it appears that a complex set of computations, including filtering and integration, as well as summation of input, occurs prior to formation of the response.

E. Future Work

This model of control of balance appears to serve as an ideal framework for studying responses to ambiguous sensory input. This framework must be tested with additional experiments similar to the preliminary trials described in Section IV. Such experiments will reveal limitations to this model and indicate areas in which additional complexity is required.

The model can also be used to study integration of sensory information. Experiments in posture have explored alteration of visual, proprioceptive, and vestibular input in conjunction with platform perturbations [15]. Modeling can be used to predict and explain many types of behavior arising from such altered sensory input conditions.

The LQG controller can be used to study how system performance is related to the precision of sensors. One approach would be to describe the signal-to-noise ratio or precision of each sensor with a power spectral density matrix. The linear system with noise would then be modeled as a Gauss-Markov random process [6], which can be used to predict the covariance of the output states. Thus, loss of sensory input could be modeled to calculate increases in uncertainty of the state. Certain elements of the state estimate are affected by some sensors more than others, so that a ranking of importance could be established in terms of the amount a particular sensor is relied upon in formation of the estimate.

With age, various components of the neuro-musculo-skeletal system are presumed to degrade [15]. Sensor noise, transmission delays, and actuator weakness may all increase in the elderly. In addition, the internal model of the system and the control may or may not adapt accordingly. The effects of such adaptation may also be modeled in the LQE and LQR components, so that predictions can be made to test hypotheses concerning the process of aging or the effects of disease or trauma affecting sensors.

VI. Conclusion

This work demonstrates first that biomechanics and task requirements place substantial constraints on the set of meaningful choices available to the CNS when it is faced with the necessity of stabilizing the body. Second, the multilink dynamics dictate not only feasibility, but also ease of achieving certain combinations of joint angular accelerations. Third, the decisions remaining to the CNS appear to be made so as to preserve upright balance while maintaining an economy of movement.

The proposed model therefore combines elements of biomechanics and sensor-based control and serves as a framework for studying motor control objectives and constraints relevant to the CNS. Aside from the formulation of objectives, it serves as a convenient method for producing feedback gains that can be used in control systems analyses to test motor control hypotheses within a structure that is compatible with a number of existing models and theories (e.g., [3], [9]). Finally, the integration of sensory input provides predictive and analytic capabilities that are useful for studying sensory processing and changes to the system.

Appendix A

The LQG controller is formed by augmenting the model of (11) with sensor dynamics, and then selecting weighting matrices for the linear quadratic estimator. Together, the estimator and regulator form the full LQG controller. Loop transfer recovery can be applied to adjust for loss of robustness in the estimator-based controller [8].

A. Inclusion of Sensor Dynamics

Sensor dynamics are integrated into the system equations of form (7) if written in the form

$$\dot{x}_s = A_s x_s + B_s u_s \tag{A.1a}$$

$$y_s = C_s x_S + D_s u_s \tag{A.1b}$$

where the sensor inputs are defined as $u_s \equiv x_r$. The complete system equations are put in the form of (7) by

$$x = \begin{bmatrix} x_r \\ x_s \end{bmatrix}, \quad y = y_s, \quad u = u_r \tag{A.2a}$$

$$A = \begin{bmatrix} A_r & 0 \\ B_s & A_s \end{bmatrix}, \quad B = \begin{bmatrix} B_r \\ 0 \end{bmatrix},$$

$$C = [D_s \quad C_s], \quad D = 0 \tag{A.2b}$$

where y_s is the sensory output available to the CNS.

B. Weighting Matrices for Linear Quadratic Estimator

The gains for the optimal state estimator are determined by the power spectral density matrices W and V of (7). Given a reasonably accurate internal model and initial conditions, computer simulations of an LQG system without injection of noise

give accurate state estimates, rendering implementation of the filter necessary only for prediction of state covariance matrices, which describe the probable deviations from expected values. The certainty-equivalence principle [6] also guarantees that the LQR can be designed independently of the LQG. Therefore, the state estimator is designed and implemented based on (8).

Note that the estimator can also be used to model direct feedthrough of sensory measurements as in [10] by rendering the internal model unreliable. This is done by increasing its uncertainty (process noise w), so that the state estimator then depends purely on sensors. The resulting covariance matrices can be compared to those computed with an internal model to determine the performance of the system with and without an internal model.

APPENDIX B

The gain matrix K_r of (17) is linearly related to parameter σ. This is shown by noting that

$$K_r = R^{-1}B_r^T S \tag{B.1}$$

where S is the stable steady-state solution to the Riccati equation

$$\dot{S} = -A_r^T S - SA_r + SB_r R^{-1} B_r^T S - \sigma^2 Q = 0 \tag{B.2}$$

as described in [6]. Defining

$$Z \equiv B_{r2} R^{-1} B_{r2}^T$$

and rewriting (B.2) in block form combined with (15) produces

$$-\begin{bmatrix} 0 & S_{11} \\ 0 & S_{21} \end{bmatrix} - \begin{bmatrix} 0 & 0 \\ S_{11}^T & S_{21}^T \end{bmatrix} + \begin{bmatrix} S_{21}^T Z S_{21} & S_{21}^T Z S_{22} \\ S_{22}^T Z S_{21} & S_{22}^T Z S_{22} \end{bmatrix} - \begin{bmatrix} \sigma^2 Q_{11} & 0 \\ 0 & 0 \end{bmatrix} = 0. \tag{B.3}$$

Rearranging terms reveals

$$\begin{bmatrix} \sigma^2 Q_{11} & S_{11} \\ S_{11}^T & S_{21} + S_{21}^T \end{bmatrix} = \begin{bmatrix} S_{21}^T Z S_{21} & S_{21}^T Z S_{22} \\ S_{22}^T Z S_{21} & S_{22}^T Z S_{22} \end{bmatrix}, \tag{B.4}$$

the upper-left block of which shows that solutions for S_{21} are linear in σ. The lower-right block of (B.4) shows that S_{22} is therefore linear in $\sqrt{\sigma}$.

Writing (B.1) as

$$K_r = R^{-1}[0 \; B_{r2}^T] \begin{bmatrix} S_{11} & S_{21}^T \\ S_{21} & S_{22} \end{bmatrix} = R^{-1} \cdot B_{r2}^T \cdot [S_{21} \quad S_{22}] \tag{B.5}$$

leads directly to (17).

ACKNOWLEDGMENT

Special thanks to F. E. Zajac, W. S. Levine, G. E. Loeb, and C. F. Runge for their insightful comments and suggestions concerning this manuscript. C. F. Runge also offered invaluable assistance in data collection.

REFERENCES

[1] J. H. J. Allum, F. Honegger, and C. R. Pfaltz, "The role of stretch and vestibulo-spinal reflexes in the generation of human equilibriating reactions," in *Afferent Control of Posture and Locomotion, Progress in Brain Research*, O. Pompeiano and J. H. J. Allum, Eds. Amsterdam: Elsevier, 1989.

[2] J. H. J. Allum, E. A. Keshner, F. Honegger, and C. R. Pfaltz, "Organization of leg-trunk-head equilibrium movements in normals and patients with peripheral vestibular deficits," in *Vestibulospinal Control of Posture and Locomotion, Progress in Brain Research*, O. Pompeiano and J. H. J. Allum, Eds. Amsterdam: Elsevier, 1988.

[3] K. Barin, "Evaluation of a generalized model of human postural dynamics and control in the sagittal plane," *Biol. Cyber.*, vol. 61, pp. 37–50, 1989.

[4] M. F. Bobbert and G. J. van Ingen Schenau, "Coordination in vertical jumping," *J. Biomech.*, vol. 21, pp. 249–262, 1988.

[5] J. Borah, L. R. Young, and R. E. Curry, "Optimal estimator model for human spatial orientation," in *Representation of Three-Dimensional Space in the Vestibular, Oculomotor, and Visual Systems*, V. Henn and B. Cohen, Eds. New York: The New York Academy of Sciences, 1988.

[6] A. E. Bryson and Y.-C. Ho, *Applied Optimal Control*. Washington, D.C.: Hemisphere Publ. Corp., 1975.

[7] P. C. Camana, H. Hemami, and C. W. Stockwell, "Determination of feedback for human posture control without physical intervention," *J. Cyber.*, vol. 7, pp. 199–225, 1977.

[8] J. C. Doyle and G. Stein, "Robustness with observers," *IEEE Trans. Automat. Contr.*, vol. AC-24, pp. 607–611, 1979.

[9] C. L. J. Golliday and H. Hemami, "Postural stability of the two-degree-of-freedom biped by general linear feedback," *IEEE Trans. Automat. Contr.*, vol. AC-21, pp. 74–79, 1976.

[10] J. He, W. S. Levine, and G. E. Loeb, "Feedback gains for correcting small perturbations to standing posture," *IEEE Trans. Automat. Contr.*, vol. 36, pp. 322–332, 1991.

[11] H. Hemami and A. Katbab, "Constrained inverted pendulum model of evaluating upright postural stability," *J. Dyn. Sys. Meas. Cont.*, vol. 104, pp. 343–349, 1982.

[12] H. Hemami and B. T. Stokes, "A qualitative discussion of mechanisms of feedback and feedforward in the control of locomotion," *IEEE Trans. Biomed. Eng.*, vol. BME-30, pp. 681–688, 1983.

[13] H. Hemami, F. C. Weimer, C. S. Robinson, C. W. Stockwell, and V. S. Cvetkovic, "Biped stability considerations with vestibular models," *IEEE Trans. Automat. Contr.*, vol. AC-23, pp. 1074–1079, 1978.

[14] F. B. Horak and L. M. Nashner, "Central programming of postural movements: Adaptation to altered support-surface configurations," *J. Neurophys.*, vol. 55, pp. 1369–1381, 1986.

[15] F. B. Horak, L. M. Nashner, and H. C. Diener, "Postural strategies associated with somatosensory and vestibular loss," *Exp. Brain Res.*, vol. 82, pp. 167–177, 1990.

[16] G. A. Horstmann and V. Dietz, "A basic posture control mechanism: The stabilization of the centre of gravity," *Electroenceph. Clin. Neurophys.*, vol. 76, pp. 165–176, 1990.

[17] T. Kailath, *Linear Systems*. Englewood Cliffs, NJ: Prentice-Hall, 1980.

[18] M. Kawato, "Computational schemes and neural network models for formation and control of multijoint arm trajectory," in *Neural Networks for Control*. Cambridge, MA: MIT Press, 1990.

[19] A. D. Kuo and F. E. Zajac, "A biomechanical analysis of muscle strength as a limiting factor in standing posture," *J. Biomech.*, vol. 26, suppl. 1, pp. 137–150, 1993.

[20] ——, "Human standing posture: Multijoint movement strategies based on biomechanical constraints," in *Progress in Brain Research*, J. H. J. Allum, D. J. Allum-Mecklenburg, F. P. Harris, and R. Probst, Eds. Amsterdam: Elsevier, 1993, vol. 97, pp. 349–358.

[21] ——, "What is the nature of the feedforward component in motor control?" *Behav. Brain Sci.*, vol. 15, p. 767, 1992.

[22] G. E. Loeb, W. S. Levine, and J. He, "Understanding sensorimotor feedback through optimal control," in *Cold Spring Harbor Sympos. Quant. Biol.*, vol. 55, pp. 791–803, 1990.

[23] J. Massion, "Movement, posture and equilibrium: Interaction and coordination," *Prog. Neurobiol.*, vol. 38, pp. 35–56, 1992.

[24] G. McCollum and T. K. Leen, "Form and exploration of mechanical stability limits in erect stance," *J. Motor Behav.*, vol. 21, pp. 225–244, 1989.

[25] L. M. Nashner, "Organization and programming of motor activity during posture control," in *Reflex Control of Posture and Movement, Progress in Brain Research*, R. Granit and O. Pompeiano, Eds. Elsener, North Holland: Biomedical Press, 1979.

[26] L. M. Nashner and G. McCollum, "The organization of human postural movements: A formal basis and experimental synthesis," *Behav. Brain Sci.*, vol. 8, pp. 135–172, 1985.
[27] C. C. Ormsby and L. R. Young, "Integration of semicircular canal and otolith information for multisensory orientation stimuli," *Math. Biosci.*, vol. 34, pp. 1–21, 1977.
[28] M. G. Pandy, F. E. Zajac, E. Sim, and W. S. Levine, "An optimal control model for maximum-height human jumping," *J. Biomech.*, vol. 23, pp. 1185–1198, 1990.
[29] D. A. Robinson, "Implications of neural networks in how we think about brain function," *Behav. Brain Sci.*, vol. 15, pp. 644–655, 1992.
[30] D. E. Rumelhart, J. L. McLelland, and P. R. Group, *Parallel Distributed Processing: Explorations in the Microstructure of Cognition*. Cambridge: MIT Press, 1988.
[31] A. H. Seif-Naraghi and J. M. Winters, "Variations in neuro-control strategies with scaling of optimization criteria," in *10th Annu. Int. Conf. IEEE Eng. Med. & Biol. Society*, 1988.
[32] C. S. Sherrington, "Flexion-reflex of the limb, crossed extension reflex and reflex stepping and standing," *J. Physiol.*, vol. 40, pp. 28–121, 1910.
[33] R. F. Stengel, *Stochastic Optimal Control*. New York: Wiley-Interscience, 1986.
[34] J. M. Winters, "Hill-based muscle models: A systems engineering perspective," in *Multiple Muscle Systems: Biomechanics and Movement Organization*, J. M. Winters and S.-L. Y. Woo, Eds. New York: Springer-Verlag, 1990.
[35] F. E. Zajac, "Muscle and tendon: Properties, models, scaling, and application to biomechanics and motor control," in *Critical Reviews in Biomedical Engineering*, G. L. Gottlieb, Ed. Boca Raton, FL: CRC Press, Inc., 1989.

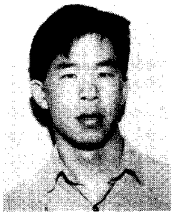

Arthur D. Kuo (S'85–M'93) received the B.S. degree in electrical engineering from the University of Illinois at Urbana-Champaign in 1987. At Stanford University, he received the M.S. degree in 1989, and the Ph.D. in 1993, both in mechanical engineering.

From 1993 to 1994, he served as a Postdoctoral Fellow at the R. S. Dow Neurological Sciences Institute in Portland, OR. In 1994, he joined the faculty of the Department of Mechanical Engineering and Applied Mechanics at the University of Michigan in Ann Arbor. His interests are in control theory, dynamics, convex geometry, and optimization, and in the application of those areas to human motor control and biomechanics.